

Supplementary Information

Using a stable protein scaffold to display peptides that bind to alpha-synuclein fibrils

Samuel Bismut^{1,4}, Matthias M. Schneider^{2,4}, Masashi Miyasaki¹, Yuqing Feng³, Ellis J. Wilde¹, M. Dylan Gunawardena¹, Tuomas P.J. Knowles², Gabrielle S. Kaminski Schierle³, Laura S. Itzhaki¹ and Janet R. Kumita^{1,*}

¹Department of Pharmacology, University of Cambridge, Tennis Court Road, Cambridge, UK, CB2 1PD

²Yusuf Hamied Department of Chemistry, University of Cambridge, Lensfield Road, Cambridge, UK, CB2 1EW

³Department of Chemical Engineering and Biotechnology, University of Cambridge, Cambridge, UK, CB3 0AS

⁴These authors contributed equally

*To whom correspondence should be addressed: jrk38@cam.ac.uk

Table S1: Protein sequences and mass spectrometry analysis

Amino acid sequences for the different CTPR variants show a solvating helix (blue) and an N-terminal His-tag at the N-terminus (italics). Fibril-binding motifs are shown in bold/italics and they are flanked by DPNN linker regions (underlined).

| Protein | Amino acid sequence | Expected Mass (Da) | Observed Mass (Da) |
|-------------------|---|--------------------|--------------------|
| CPTR3 | MRGSHHHHHHGLVPRGSAEAWYNLGNAYY KQGDYQKAIEYYQKALELDP R SAEAWYNLG NAYYKQGDYQKAIEYYQKALELDP R SAEAW YNLGNAYYKQGDYQKAIEYYQKALELDP R S A <u>EAQNLGN AKQKQG</u> | 15633.2 | 15633.2 ± 1.0 |
| Cys-CTPR3 | MRGSHHHHHHGLVPRGCAEAWYNLGNAYY KQGDYQKAIEYYQKALELDP R SAEAWYNLG NAYYKQGDYQKAIEYYQKALELDP R SAEAW YNLGNAYYKQGDYQKAIEYYQKALELDP R S A <u>EAQNLGN AKQKQG</u> | 15649.2 | 15648.6 ± 0.2 |
| FibSyn-CTPR3 | MRGSHHHHHHGLVPRGSAEAWYNLGNAYY KQGDYQKAIEYYQKALELDP NN <u><i>KL VFFAEDP</i></u> <u>NN</u> AEAWYNLGNAYYKQGDYQKAIEYYQKAL ELDPR SAEAWYNLGNAYYKQGDYQKAIEYY QKALELDP R S <u>EAQNLGN AKQKQG</u> | 16893.6 | 16892.6 ± 0.7 |
| Cys-FibSyn-CTPR3 | MRGSHHHHHHGLVPRGCAEAWYNLGNAYY KQGDYQKAIEYYQKALELDP NN <u><i>KL VFFAEDP</i></u> <u>NN</u> AEAWYNLGNAYYKQGDYQKAIEYYQKAL ELDPR SAEAWYNLGNAYYKQGDYQKAIEYY QKALELDP R S <u>EAQNLGN AKQKQG</u> | 16909.6 | 16915.3 ± 6.0 |
| FibSyn2-CTPR3 | MRGSHHHHHHGLVPRGSAEAWYNLGNAYY KQGDYQKAIEYYQKALELDP NN <u><i>KL VFWAKD</i></u> <u>PNN</u> AEAWYNLGNAYYKQGDYQKAIEYYQKA LELDP R SAEAWYNLGNAYYKQGDYQKAIEY YQKALELDP R S <u>EAQNLGN AKQKQG</u> | 16931.6 | 16931.7 ± 0.1 |
| Cys-FibSyn2-CTPR3 | MRGSHHHHHHGLVPRGCAEAWYNLGNAYY KQGDYQKAIEYYQKALELDP NN <u><i>KL VFWAKD</i></u> <u>PNN</u> AEAWYNLGNAYYKQGDYQKAIEYYQKA LELDP R SAEAWYNLGNAYYKQGDYQKAIEY YQKALELDP R S <u>EAQNLGN AKQKQG</u> | 16947.7 | 16947.7 ± 0.2 |
| CTPR4 | MRGSHHHHHHGLVPRGSAEAWYNLGNAYY KQGDYQKAIEYYQKALELDP NN AEA WYNLG NAYYKQGDYQKAIEYYQKALELDP NN AEA W YNLGNAYYKQGDYQKAIEYYQKALELDP NN A EA WYNLGNAYYKQGDYQKAIEYYQKALELDP PNN | 18048.6 | 18054.8 ± 6.7 |
| Cys-CTPR4 | MRGSHHHHHHGLVPRGCAEAWYNLGNAYY KQGDYQKAIEYYQKALELDP NN AEA WYNLG NAYYKQGDYQKAIEYYQKALELDP NN AEA W YNLGNAYYKQGDYQKAIEYYQKALELDP NN A | 18064.7 | 18066.5 ± 2.8 |

| | | | |
|----------------------------|---|---------|------------------|
| | EAWYNLGNAYYKQGDYQKAIEYYQKALELD PNN | | |
| 2XFibSyn- CTPR4 | MRGSHHHHHHGLVPRGSAEAWYNLGNAYY KQGDYQKAIEYYQKALELD <u>PNNKLVFFAEDP</u> <u>NNAEAWYNLGNAYYKQGDYQKAIEYYQKAL</u> ELDPNNAEAWYNLGNAYYKQGDYQKAIEYY QKALELD <u>PNNKLVFFAEDP</u> NNAEAWYNLGN AYYKQGDYQKAIEYYQKALELDPNN | 20599.5 | 20599.0 ± 2.0 |
| Cys- 2XFibSyn- CTPR4 | MRGSHHHHHHGLVPRGCAEAWYNLGNAYY KQGDYQKAIEYYQKALELD <u>PNNKLVFFAEDP</u> <u>NNAEAWYNLGNAYYKQGDYQKAIEYYQKAL</u> ELDPNNAEAWYNLGNAYYKQGDYQKAIEYY QKALELD <u>PNNKLVFFAEDP</u> NNAEAWYNLGN AYYKQGDYQKAIEYYQKALELDPNN | 20615.6 | 20615.6 ± 0.2 |

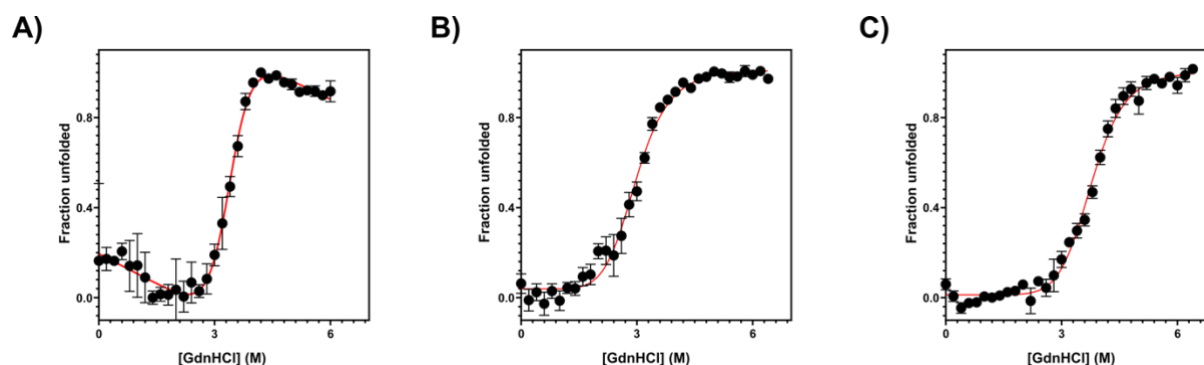


Fig. S1. GdnHCl-induced denaturation of CTPR proteins. Purification of CTPR variants yielded samples with concentrations between 150-400 μ M. A) FibSyn-CTPR3, B) FibSyn2-CTPR3 and C) 2XFibSyn-CTPR4CTPR4. 1 μ M of protein in 50 mM sodium phosphate, 150 mM NaCl, pH 7.5 and increasing GdnHCl concentrations (from 0 M to 6.4 M) at 25°C. Excitation was at 295 nm and emission intensity was measured at 360 nm. A minimum of three independent experiments were recorded for each protein. The data were fitted with a two-state model to give the midpoint of unfolding and m value (a constant proportional to the change in solvent-accessible surface area upon unfolding). Error bars show the standard error of the mean.

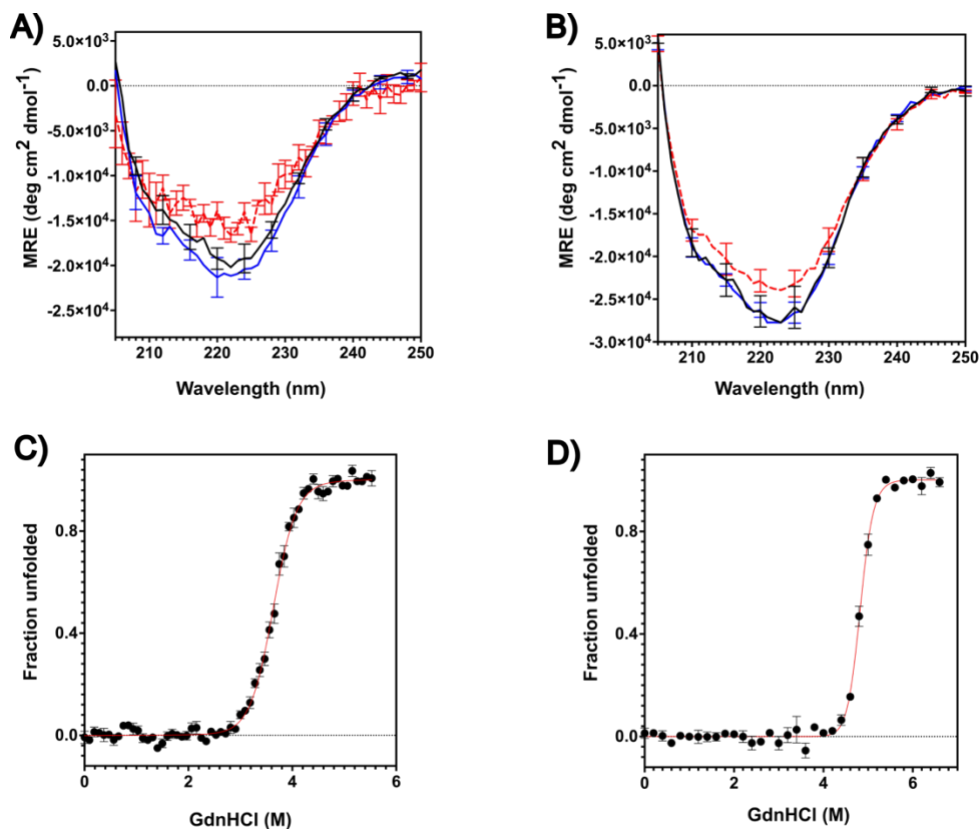


Fig. S2. CD analysis and GdnHCl-induced denaturation of CTPR3 and CTPR4 (negative controls). To determine whether fibril-binding is due to the presence of the peptide motifs, CTPR3 and CTPR4 containing the native inter-repeat loops were used. CD analysis of A) CTPR3 and B) CTPR4 was performed with 5 μ M of protein in 50 mM sodium phosphate, 150 mM NaCl, 0.5 mM TCEP, pH 7.5, spectra recorded from 205 nm to 250 nm in 0.5 nm intervals. Samples were measured at 20°C (black), 90°C (red) and return to 20°C (blue). GdnHCl denaturation was performed for C) CTPR3 and D) CTPR4 with 1 μ M of protein in 50 mM sodium phosphate, 150 mM NaCl, pH 7.5 and increasing GdnHCl concentration (from 0 M to 6.4 M) at 25°C. Excitation was at 295 nm and emission intensity was measured at 360 nm. A minimum of three independent experiments were recorded for each protein. The data were fitted to a two-state model to give the midpoint of unfolding and m value (a constant proportional to the change in solvent-accessible surface area upon unfolding). Error bars show the standard error of the mean

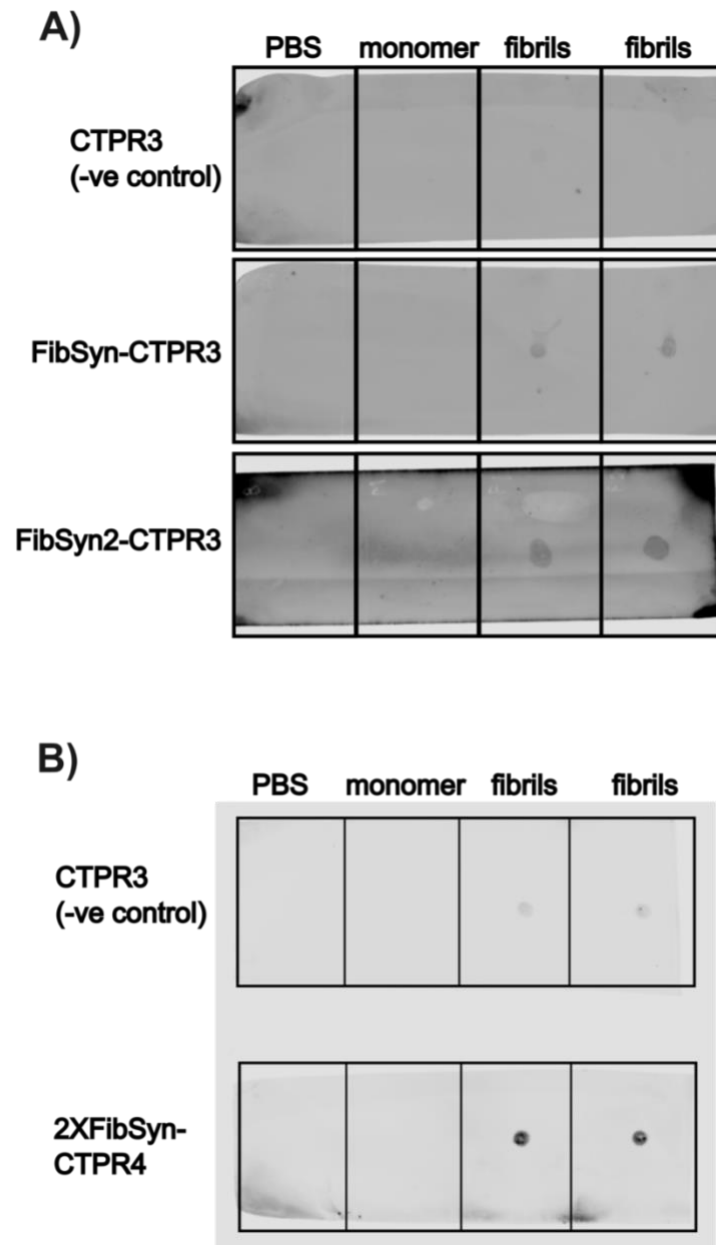


Fig. S3. Dot blot assay to test CTPR variant binding to monomeric and fibrillar α -synuclein. Monomeric and fibrillar α -synuclein samples were applied to nitrocellulose membranes followed by incubation with A) Alexa FluorTM 594-labelled CTPR variants and B) Alexa FluorTM 647-labelled CTPR variants. Imaging using a LiCor Odessey system shows no interactions between the fluorophore-labelled CTPRs and monomeric α -synuclein and increased interactions between fibrillar α -synuclein and CTPR variants containing the fibril-binding peptide motifs. Some non-specific binding was observed with the Alexa FluorTM 647-labelled CTPR3 negative control (also observed in the fibril-pulldown assay), this non-specific binding was not observed with the Alexa FluorTM 594-labelled CTPR3 negative control.

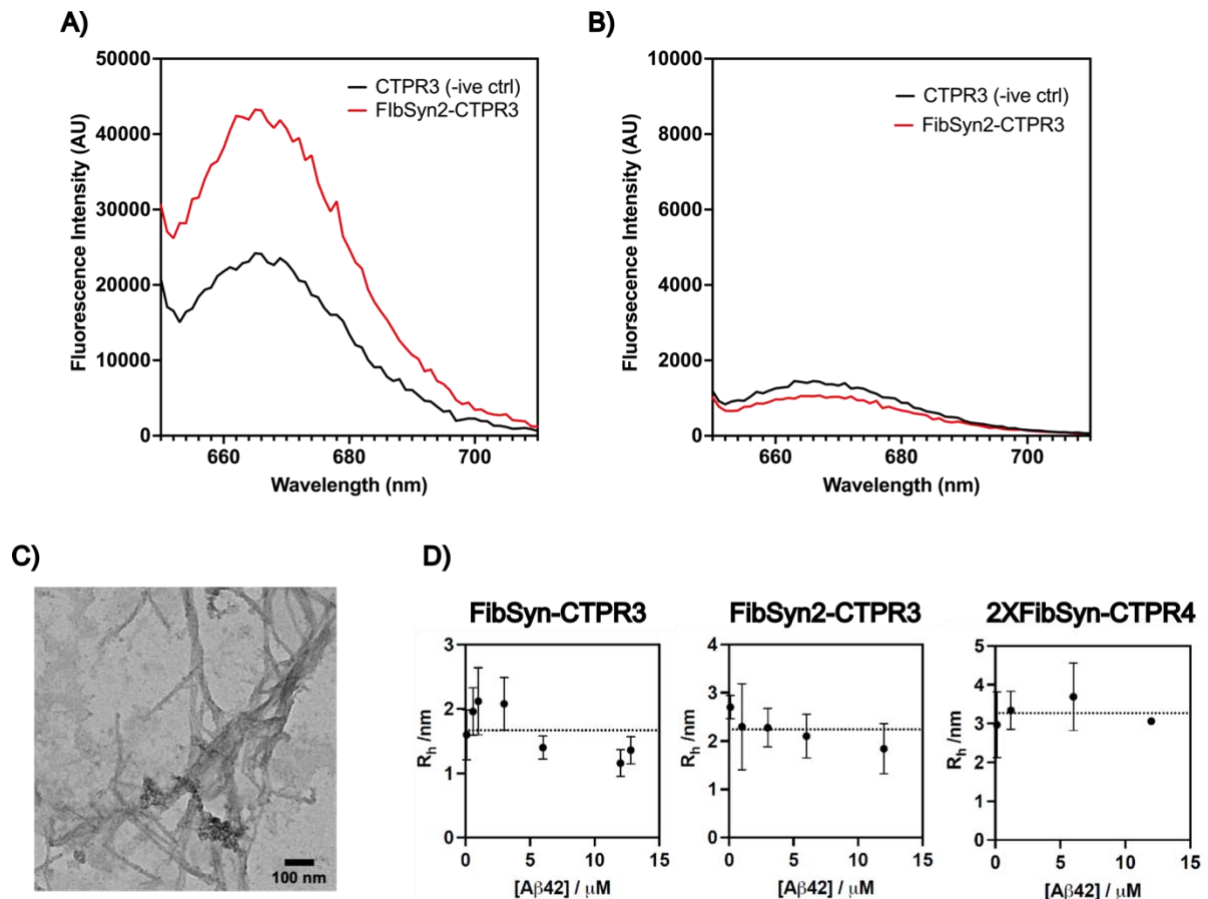


Fig S4. Comparing CTPR variants interactions with α -synuclein fibrils versus $A\beta_{1-42}$ fibrils. A) Fluorescence emission spectrum for CTPR3 (negative control) and FibSyn-CTPR3 bound α -synuclein fibrils showing specific interactions. B) Fluorescence emission spectrum for CTPR3 (negative control) and FibSyn-CTPR3 bound $A\beta_{1-42}$ fibrils, showing no specific interactions with FibSyn-CTPR3. C) Representative TEM image of $A\beta_{1-42}$ fibrils used for fibril pull-down and MDS assays. D) MDS assays of Alexa Fluor™ 647-labelled CTPR variants with increasing concentrations of $A\beta_{1-42}$ fibrils. No change in hydrodynamic radius is seen for any of the FibSyn-CTPRs.